ISSN: 0974-5335
IJLST (2017), 10(1):1-13

Mining disease information in low-molecular-weight serum proteins based on nanoporous silicon micro-flake and mass spectrometry

Farid Abu Shammala
Adjunct professor of Analytical Chemistry, Department of Pharmacology, University of Palestine, Gaza, PALESTINE
drfaridshammala@hotmail.com

ABSTRACT:
Here, we developed and characterized a sol gel-derived mesoporous silica thin films, with tunable features at the nanoscale, they were fabricated using the triblock copolymer template pathway. With the use of different polymer templates and polymer concentrations in the precursor solution, various pore size distributions, pore structures, connectivity and surface properties were determined and applied for selective recovery of low mass proteins. The selective parsing of the enriched peptides into different subclasses according to their physicochemical properties will enhance the efficiency of recovery and detection of low abundance species. These films are structurally characterised by electron microscope (EM) and X-ray dispersion (XRD) . It has been found that with tunable pore dimension, pore texture, and surface properties, the mesoporous films are the perfect tools for proteomics preconcentration. The use of triblock copolymer template pathway allows large proteins not enter the pore size of the mesoporous films and to be washed out of serum samples. Allowing various LMW proteins to inter and trapped inside various pore size and pore structure distributions. We also predicted that acetonitrile (CAN) would cause many smaller proteins to dissociate from their carrier molecules, mainly albumin. The eluted LMW proteins samples with ACN were analyzed using matrix- assisted laser desorption/ionization time-of-flight mass spectrometry (MALDI-TOF MS). The results shown to be a significant potential for the discovery of proteomic biomarkers for cancer. By utilizing this method, we identified 559 (n = 2) proteins belonged to LMW proteins. Furthermore, this mesoporous films are perfect tools for proteomics preconcentration and analysis, could identify 67.4% and 39.8% more LMW proteins than that in representative methods of glycine SDS-PAGE and optimized-DS, respectively. These results demonstrate that the mesoporous silicas method offers a rapid, highly reproducible and efficient approach for screening biomarkers from serum through proteomic analyses.

Keywords: MALDI-TOF MS, mesoporous silica, proteomics, low molecular weight, proteome.

INTRODUCTION

Serum potentially carries an archive of important histological information whose determination could serve to improve early disease detection. The analysis of serum, however, is analytically challenging due to the high dynamic concentration range of constituent protein/peptide species, necessitating extensive fractionation prior to mass spectrometric analyses. The low molecular weight (LMW) serum proteome is that protein/peptide fraction from which high molecular weight proteins, such as albumin, immunoglobulins, transferrin, and lipoproteins, have been removed. This LMW fraction is made up of several classes of physiologically important proteins such as cytokines, chemokines, peptide hormones, as well as proteolytic fragments of larger proteins.Many diseases, such as cancer, do not show obvious clinical symptoms until the disease is in advanced stages and difficult to treat successfully. Detection of such diseases in early stages can greatly reduce disease-related mortality. Serum potentially carries an archive of important histological information whose determination could serve to improve early cancer detection. The analysis of serum, however, is analytically challenging due to the high dynamic concentration range of constituent protein/peptide species, necessitating extensive fractionation prior to mass spectrometric analyses. The low molecular weight ((LMW, molecular weight ≤ 30kDa)) serum proteome is that protein/peptide fraction from which high molecular weight proteins, such as albumin, immunoglobulins, transferrin, haptoglobulin and lipoproteins, have been removed.

The high complexity of protein fragments in plasma potentially offer large amounts of information of pathophysiologic significance that may be applied for diagnostic purposes. Recently, new evidence has revealed that the low-molecular weight region of the circulatory proteome is a rich and untapped source of potential diagnostic biomarkers (1, 2). However, detection of LMWP in complex serum samples by MALDI-TOF MS still face challenges since the components of high abundance generally dominate the spectrum and tend to suppress detection of lower abundance proteins or its fragments.

The human serum proteome has been extensively screened for biomarkers. To detect diseases early in the general population, new diagnostic approaches are needed that have adequate sensitivity and specificity. Recent studies have used mass spectrometry to identify a serum proteomic pattern for breast and ovarian cancer. Serum contains 60–80 mg/mL protein, but 57–71% of this is serum albumin, and 8–26% are γ-globulins. These large proteins must be depleted before smaller, less-abundant proteins can be detected using mass spectrometry, but because serum albumin is known to act as a carrier for smaller proteins, removal of these molecules using different techniques such as columns separation or filtration techniques may result in the loss of molecules of interest. Mass spectrometry-based analyses of the low-molecular-weight fraction of serum proteome allow identifying proteome profiles that are potentially useful in detection and classification of cancer. Several published studies have shown that multipeptide signatures selected in numerical tests have potential values for diagnostics of different types of cancer. However due to apparent problems with standardization of methodological details, both experimental and computational, none of the proposed peptide signatures analyzed directly by MALDI/SELDI-TOF spectrometry has been approved for routine diagnostics (3). Noteworthy, several components of proposed cancer signatures, especially those characteristic for advanced cancer, were identified as fragments of blood proteins involved in the acute phase and inflammatory response. Techniques such as 2-dimensional gel electrophoresis and multidimensional liquid chromatography can remove signal-suppressing components of complex biological mixtures such as serum or cell extracts (4–8), but these techniques are laborious and time-consuming. In a new pretreatment method, serum peptides are fractionated and concentrated on surface-modified targets with specific protein-capture properties. The first clinical investigations using SELDI-TOF MS for different cancer types (e.g., ovarian, prostate, bladder, breast, lung, and brain) revealed high diagnostic sensitivities and specificities (9–16). However, for the same cancers, different patterns were identified by various research groups using the same types of biological spec-imens and the same analytical platform (17). These discrepancies could be attributable to poorly defined preanalytical protocols. For accurate MS analysis, the proteome fractionation procedure and the preanalytical conditions for proteome mapping must be carefully assessed (18). The aim of this study was to establish a well-defined protocol for precise proteome analysis and preanalytical to minimize the variability in data obtained for the proteome pattern. We used a novel sample pretreatment procedure with nanoporous silica thin films before identification of human serum proteome profiles using MALDI-TOF MS (19).

The development of porous nanomaterials, with controllable features offering advantageous new physico-chemical properties, has widely improved the use of nanotechnology in biomedical application (20).Studies on ordered mesoporous materials have attracted extensive attention since the discovery of the M41S family of mesoporous silicas in 1992 (21, 22). These M41S materials, exhibiting high surface area and volume, were formed by following the sol-gel method with an ionic surfactant (cetyltrimethylammonium bromide) as template. In this kind of materials the average pore size extends over the micro-to mesopore range. In addition, the concept of “template” was first postulated in the synthesis of esoporous silicate materials (23). Among these SBA-type silica materials, SBA-16 is considered a very interesting mesostructure due to the fact it has a 3D cubic arrangement of mesopores corresponding to the Im3m space group. Polyethylene oxide-polypropylene oxide-polyethylene oxide (PEO-PPO-PEO) triblock copolymers are a subset of amphiphilic block polymers known commercially as Pluronic surfactants. A variety of Pluronic surfactants are readily available, with differing block and arm lengths. These triblock copolymers with relatively large poly(ethylene oxide) (PEO) chains, such as Pluronic F127, F108, and F98, can serve as templates, but templates with very long PEO chains, such as F88 (EO104PO39EO104) and F68 (EO76PO29EO76), are seldom used due to the strict conditions necessary to obtain high-quality SBA-16 (24). In addition, the mesophase can be created using mixtures of Pluronic P123 and Pluronic F127 templates or in a ternary water, butanol and Pluronic F127 system. The structure of SBA-16 can be described by a triply periodic minimal surface of I-WP (body centered, wrapped package) (25).

This nanotechnology provides a powerful tool that will lead to the successful discovery of novel biomarkers with potential significant clinical utility to early diagnosis and manage various diseases. One of the advantages of our work is that the procedure demonstrated the conservation and the long-term stability of low-molecular-weight proteins in the porous matrix of the MSC and evaluated the efficiency and reproducibility of this technology.

METHODS

Chemicals: Gradient-grade Tetraethyl orthosilicate (TEOS) and cetyl trimethylammonium bromide (CTAB) were purchased from Sigma Chemicals . Ethanol and HCl was purchased from Fisher Scientific. Nonionic surfactants (F127, P123 and L121) were (Aldrich, purity 99%). All chemicals and reagents were used as received without further purification.

Preparation of mesoporous silica thin films: A typical preparation of the coating sol is as follows. Fourteen milliliters of tetraethyl orthosilicate was dissolved in a mixture of 17 ml of ethanol, 6.5 ml of distilled water and 0.5 ml of 2M HCl and stirred for 1 h at 80◦C to form a clear silicate solution. Separately, 1.8 g of Pluronic F-127 was dissolved in 10 ml of ethanol by stirring at room temperature. The coating solution was prepared by mixing the silicate solution into the triblock copolymer solution followed by stirring of the resulting solution for 2 h at room temperature. The pH of the mixture solution remained around 1.5. The coating sol was deposited on a Si (100) wafer by spin-coating at the spin rate of 2000 r.p.m. for 20 s. To increase the degree of polymerization of the silica framework in the films and to further improve their thermal stability, the films were heated at 80◦C for 12 h. They were then calcinated at 425◦C to remove the organic surfactant. The temperature was raised at a rate of 1◦C min−1, and the furnace was heated at 425◦C for 5 h. hydrolyzed silicate sol was dropped into the triblock co-polymer solution followed by stirring for 2 hrs at room temperature. The coating sol was spin coated on a Si (1 0 0) wafer for 25 seconds at the spin rate of 750 rpm for the solution containing CTAB, 1500 rpm for the solution with F127 or P123 and 2500 rpm for the mixture with L64, L121 or L121+PPG. The as-deposited films were heated at 80 °C for 24 hrs to increase the degree of polymerization of the silica framework and to further enhance their thermal stability. The temperature was raised at a rate of 1°C per min, and 47 the chips was heated at 425°C for 5 h to remove the organic surfactant. The films produced were transparent and crackless.

Blood samples: Blood samples from 10 healthy volunteers (5 females and 5 males; age range, 26–39 years) were collected in serum, EDTA, heparin, and citrate Monovettes. Serum and plasma aliquots were treated with TFA and ACN to each serum sample such that the final concentrations are 0.05% TFA and 5% ACN. Shake these samples on a table vortex shaker at room temperature for 30 minutes. stored in 1.5-mL polypropylene tubes. The blood samples were processed according to a standardized protocol. After sample collection, the Monovettes were incubated at room temperature (25 °C) for 30 min and centrifuged at 1400g for 10 min. The plasma and serum samples were immediately frozen in aliquots of 100 mL at 80 °C; for proteome fractionation, samples were thawed at room temperature for 15 min and processed immediately. Variations in sample pretreatment are described separately below. For precision and mass accuracy analyses, serum and plasma samples were pooled from 10 individual samples (from 5 females and 5 males).

Characterization techniques: We used several characterization techniques to study the spin-coated, nanoporous silica thin films. By employing a variable-angle spectroscopic ellipsometer (J. A.Woollam Co., M-2000DI) and modelling with COMPLETEEASE software, the thickness of the thin films and their porosities were measured in the Cauchy model and effective medium approximation (EMA) model, respectively. Ellipsometric optical quantities, the phase (D) and amplitude (j), were determined by acquiring spectra at 60◦, 65◦ and 70◦ incidence angles using wavelengths from 300 to 1800 nm. In the Cauchy model, the top layer's thickness, reflective index and model-fitted, parameters An, Bn and Cn were determined by comparing the experimental data with the model and minimizing the mean square error (usually less than 10). Using the EMA model, the films' porosities were calculated by assuming a certain volume of voids in the pure silica and setting the top layer's thickness obtained by the Cauchy model as a constant. X-ray diffraction (XRD) patterns were obtained on a Philips X'Pert-MPD system with Cu Ka radiation (45 kV, 40 mA). Scans of q–2q were recorded from all spin-coated films at 1 s and 0.001◦ steps over the angle range from 0.2◦ to 6◦. Transmission electron microscopy (TEM) and scanning transmission electron microscopy (STEM) were used to acquire micrographs of the plane view of nanoporous silica thin films with an FEI Technai (FEI Co.) at a high tension of 200 kV.

MALDI-TOF MS: For the proteome analysis, we used a linear MALDI-TOF mass spectrometer (Autoflex; Bruker Daltonics) with the following settings: ion source 1, 20 kV; ion source 2, 18.50 kV; lens, 9.00 kV; pulsed ion extraction, 120 ns; nitrogen pressure, 2.5 105 Pa. Ionization was achieved by irradiation with a nitrogen laser (337 nm) operating at 50 Hz. For matrix suppression, we used a high gating factor with signal suppression up to 500 Da. Mass spectra were detected in linear positive mode. Mass calibration was performed

with the calibration mixture of peptides and proteins in a mass range of 1000–12 000 Da. We measured 4 MALDI preparations (MALDI spots) from each magnetic bead fraction. For each MALDI spot, 300 spectra were acquired (30 laser shots at 10 different spot positions). To increase the detection sensitivity, we removed excess matrix with 6 shots at a laser power of 45% before data acquisition at 25%. All signals with a signal-to-noise (S/N) ratio 3 in a mass range of 1000–10 000 Da were recorded with use of the AutoXecute tool of the flexControl acquisition software (Ver. 2.0; Bruker Daltonics). We used the ClinProTools bioinformatics software (Ver. 1.0; Bruker Daltonics) for proteome pattern recognition.

RESULTS AND DISCUSSION

Evaluation of Pluronics for Nanoporous Silica Thin Films Approaches

Synthesis of Pluronic block copolymers is achieved using a propylene glycol initiator which is lengthened by sequential addition of propylene oxide monomer units. This reaction is catalyzed by a basic catalyst and run under elevated temperature and pressure, until the desired molecular weight is achieved. To obtain the various pore sizes required to harvest the specific proteome from serum based on size-exclusion, the polymer templates in this section were chosen from both ionic surfactant (PEO106-PPO70-PEO106 : Pluronic F127, PEO5-PPO70-PEO5: Pluronic L121). (cetyltrimethylammonium bromide: CTAB) and non-ionic triblock copolymers nanoporous silica thin film will possess a smaller pore size than the films prepared with F127 and L121, which have much higher molecular weight and provide a controlled pathway for the preparation of large-pore silicate nanostructure. N_2 adsorption-desorption measurements were conducted to determine the entrance pore size distribution and surface area of mesoporous silica thin films prepared by three different polymers. Due to the small pore size (2.01 nm) on the nanoporous silica thin film synthesized by CTAB, its sorption isotherm was Type II displaying a H1 hysteresis loop. All adsorption/desorption isotherms carried by chips prepared by non-ionic surfactants were Type IV with a well-defined H_2 hysteresis loop. As shown in figures 1, 2 the inflection points appeared at $0.30 \leq P/P0 \leq 0.80$, indicating the formation of ink-bottle shape nanopores. All results of the analysis shown that their various BJH pore sizes distributions exhibited sharp peaks, which suggested that both periodic and non-ordered nanophase were created on the chips with uniform pore size. Figure 1, is a cross-sectional TEM images of mesoporous silica thin films with different pore sizes using (a) F127 (b) P123 and (c) L121.

Our main goal was to deplete serum samples of high-abundance proteins in order to analyze the less-abundant proteins with low molecular weight (LMW, molecular weight ≤ 30kDa) serum proteome. The preconcentration method had sufficient reproducibility to allow for accurate quantitative serum proteomic analysis that differed between healthy and diseased states. The adequacy of this method was tested using MALDI-TOF-MS. Additionally, we were interested in determining best structure, type and characterization of mesoporous silica films with three different pore sizes. The transparent silica films were characterized using various methods as follows. Infrared spectroscopy was measured by a Bruker EQUINOX55 FTIR. X-ray diffraction (XRD) patterns of all mesoporous silica films were obtained on a Rigaku D/MAX-RC diffractometer with Cu Kα radiation (40 kV, 80 mA) at 0.01o step width and 1 second step time over the range $1.2\,o < 2\theta < 10o$. of mesoporous silica sol-gel that residual molecular species and their molecular weights after a precipitation procedure. Figure 2, shows XRD patterns of mesoporous silica thin films using the triblock copolymer template pathway (a) As-deposited and (b) Calcined 3-D cubic mesoporous silica thin film prepared using F127. (c) As deposited and (d) Calcined 2-D hexagonal mesoporous silica thin film prepared using P123. (e) As-deposited and (f) Calcined 3-D hexagonal mesoporous silica film prepared using L121.

The mesoporous silica (MPS) thin films with tunable features at the nanoscale, were fabricated using the triblock copolymer template pathway. The different polymer templates cause the construction of various pore size distributions, pore structures, connectivity and surface properties in the silica gel. These pore size distribution cause selective parsing of the enriched peptides into different subclasses according to their size and physicochemical properties. Thus, the pore size distribution in the mesoporous silica (MPS) thin films will enhance the efficiency of separation, recovery and detection of low abundance LMW protein species. Whereas, large proteins washed out of solution. We also predicted that this technique would cause many smaller proteins to dissociate from their carrier molecules, allowing various LMW proteins to inter and trapped inside various pore size and pore structure distributions. The LMW protein then eluted with acetonitrile (ACN). These eluted LMW proteins samples were analyzed using MALDI/SELDI-TOF spectrometry.

Analysis demonstrated reproducible results. Acetonitrile treatment clearly released many carrier-bound molecular LMW species specially albumin perior to ultrafiltration by the mesoporous silica (MPS) thin films.

The results in the studied packing arrangement of the sol-gel, have shown that majority of the ordered phases consist of cubic packing arrangements of spherical micelles, however, at very high pluronic concentrations (in the vicinity of pure polymer), lamellar phases were commonly identified. Additionally, Pluronic surfactants with a low PEO content by weight (<15%) also formed lamellar phases. As the weight percent of PEO in the molecular formula increases (~25%), hexagonal ordered phases are formed. Finally, for most pluronics with higher PEO content (>25%), cubic phases are observed. Scattering studies on these ordered phases typically demonstrate scattering rings, indicating that many randomly oriented ordered domains exist in the solution. The application of shear, however, leads to substantially enhanced ordering of the micelles, and single-crystal like scattering behavior has been observed. The phase behavior for F127 only has three major phase regions with a thin two-phase region at the interface between the isotropic phase and the cubic phase, whereas P123 has a more complicated phase diagram, including an order-to-order transition between the cubic and hexagonal phases and an extended multiphase region. Increasing the F127 concentration to 6.0×10^{-3} M yields a 3D honeycomb like nanostructure hexagonally arranged on the substrate. A further increase of the F127 concentration to 8.0×10^{-3} M resulted in a 2D hexagonal nanostructure parallel to the substrate surface.

Evaluation of Protein Preconcentration Approaches

In the blood samples, fractionation of LMO protein using nanoporous silica thin films allowed identification of 350 signals with a S/N ratio 3. Table 1. Indicate relative intensities and precision of 11 signals from the peptide/protein calibration solution and serum pool (n = 10) in the mass range 1000–10 000 Da, obtained by MALDI-TOF MS after mesoporous silica (MPS) thin films preparation. Figure 3 shows Tandem MS spectra of selected peptides identified in the proteome analysis of the LM shows proteome. Peptide enrichment using the mesoporous silica thin film chips with pluronic surfactants (F127, P123, L121).

Direct analysis of the pooled serum sample gave MALDITOF MS spectra without discrete mass signals. The reproducibility of mass spectrum generation was determined with respect to the relative peak intensities. Within-day CVs for direct MS analysis of the peptide/protein calibration mixture (without nanoporous silica thin film) were 4%–23% (data not shown), and between-day CVs were 2.8%–22%. Shown in Table 1 are the within- and between-day CVs of the relative peak intensities for 11 signals of the peptide/protein calibration mixture and of the pooled serum samples representing low, medium, and high-abundance peptides over the whole mass range after nanoporous silica thin film preconcentration and elution. Signals with relative signal intensities 2% gave within-day CVs14% and day CVs 22%. We evaluated the mass accuracy of the MS measurements , it revealed out that the maximum mass shifts over the range 1000–10 000 Da were 0.028% for the peptide/protein calibration mixture and 0.035% for the pooled serum sample. These results correlate with a variation of 1 Da in the absolute mass shift for signals 3500 Da. The detection limit for angiotensin II after direct analysis of the peptide/protein calibration mixture was 6.8 ng/L. After nanoporous silica thin films preconcentration of LMW protein, no interfering signals with S/N ratios 3 were obtained in the MALDI-TOF mass spectra in the mass range 1000–10 000 Da (data not shown). The relative intensities of the serum proteome signals changed with time after clotting. A loss of intensity with time was observed for low–molecular-mass signals (e.g., 1352.3 Da). Signals with masses 4000 Da (e.g., 4211.1 Da) increased in relative intensity with time, but signals with lower masses (e.g., 3264.2 Da) did not change in relative intensity. In samples allowed to clot for 120 min at room temperature, the background noise increased considerably (mass range 1000–2000 Da). Figure 4, Shows peptide enrichment using the mesoporous silica thin film chips with pluronic surfactants (F127, P123, L121) with different pore sizes of (a) 6.0 nm, (b) 5.0 nm, (c) 3.0 nm, and (d) 1.0 nm, respectively. MALDI MS profiles in the mass range (2000 to 18 000 Da). (e) molecular recovery when using blank nonporous silica surfaces. The results has shown that the molecular recovery is significantly reduced when using blank nonporous silica surfaces.

We compared the mass spectra of unfrozen serum aliquots with the spectra of the same samples after freezing. Unfrozen serum showed a high degree of variation in relative signal intensities, and reproducibility was poor. The same decrease was observed for signals in the mass range 3200–3300 Da (data not shown). Freezing–thawing did not affect signals for proteins/peptides1500 Da (e.g.,

1467.3 Da). In contrast, signals above 8900 Da (e.g., 8916.3, 9133.8, and 9423.8 Da) increased in relative peak intensity after only 1 freeze–thaw cycle.

The effect of pH on the recovery of LMW proteins samples from mesoporous silica thin films at different pH values, are shown in Figure 5. The best recovery is between pH 5-7 depending on the pI of the LMW protein. Figure 6, shows the stability of the LMW protein in the MPS chips with human serum, dried after washing, and stored for 3wk at room temperature. The influence of time and temperature on the proteomic analysis out of the nanoporous silica thin films, the results showed little degradation after 240 min at 4 °C and did not change for up to 120 min at 25 °C. At 40 °C, however, there was significant loss of intensity for all signals in the proteome profile after only 30 min. During a 7-day storage period at 4 °C, the relative peak intensities and the respective S/N ratios decreased after 24 h for masses 2000 Da. Signals at 3193.2 and 3264.2 Da were also affected. In contrast, we observed no change for signals with a molecular mass 4000 Da.

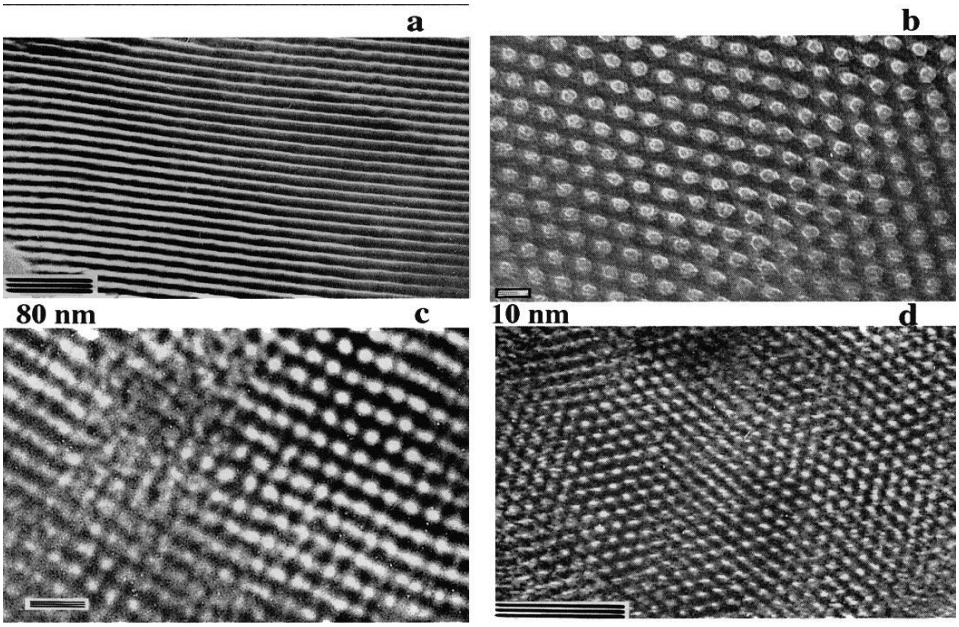

Figure 1. Cross-sectional SEM micrographs images of mesoporous silica thin films with different pore sies using (a) F127 (b) P123 (c) L121 and (d) L64.

ISSN: 0974-5335
IJLST (2017), 10(1):1-13

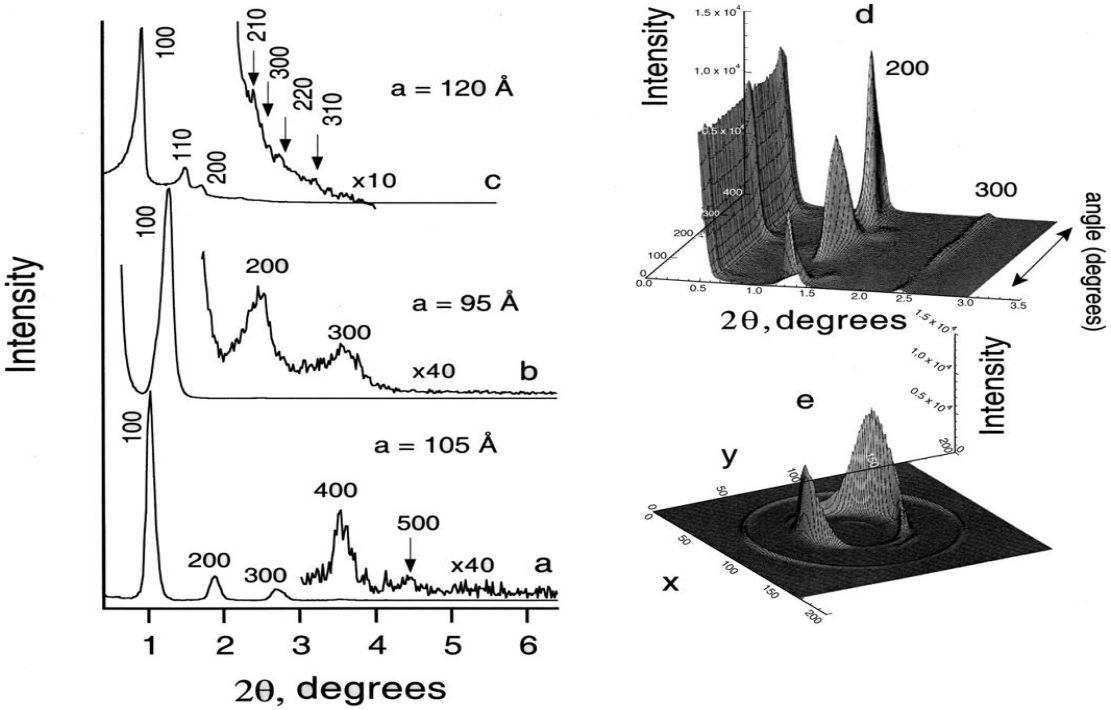

Figure 2. XRD patterns of mesoporous silica thin films using the triblock copolymer template pathway (a) As-deposited and (b) Calcined 3-D hexagonal (p6mm) mesoporous silica films prepared using amphiphilic triblock copolymer EO20PO70EO20 species (c) A bulk sample of hexagonal SBA-15 prepared using the same block copolymer at 2D XRD patterns of the as-synthesized hexagonal silica film. (d) Recorded by rotation of the film plane starting from coating direction, and (e) for different directions of the X-ray beam with respect to the film frame. The XRD patterns were acquired on a Scintag PADX diffractometer using CuKa radiation; 2D XRD patterns were recorded on Philips X'Pert Powder Diffractometer.

Table 1. Relative intensities and precision of 11 signals from the peptide/protein calibration solution and serum pool (n = 10) in the mass range 1000–10 000 Da, obtained by MALDI-TOF MS after magnetic bead preparation.

Peptide/protein calibration solution					Pooled				
	Within run		Between runs			Within run		Between runs	
Signal, m/z	Intensity	CV%	Intensity	CV%	Signal, m/z	Intensity	CV%	Intensity	CV%
1042.20	15.9	3.6	15.7	5.3	1205.91	6.4	12	5.8	17
1294.51	14.2	4.8	14.8	4.8	1355.12	6.0	5.8	6.0	5.6
1347.66	7.5	9.1	8.5	12	1468.15	12.8	7.4	14.8	14
1363.90	1.8	13	1.6	11	156.33	8.46	5.6	14	4.9
1630.88	7.9	5.8	6.8	9.6	159.50	3.4	4 .8	7.6	3.8
1482.46	4.3	12	3.1	15	2933.86	4.0	5.1	4.8	6.5
2455.73	4.2	18	1.7	23	3192.27	3.71	12	4.7	8.4
3167.61	8.2	6.5	7.3	12	3967.38	11.2	16	2.8	21
4291.45	7.4	12.3	6.5	17	4201.18	2.9	11	3.6	9.3
5746.56	5.0	8.9	3.8	14	631.42	2.7	13	2.8	22
8547.89	9.2	11	9.1	18	9130.26	1.6	14	5.6	11

ISSN: 0974-5335
IJLST (2017), 10(1):1-13

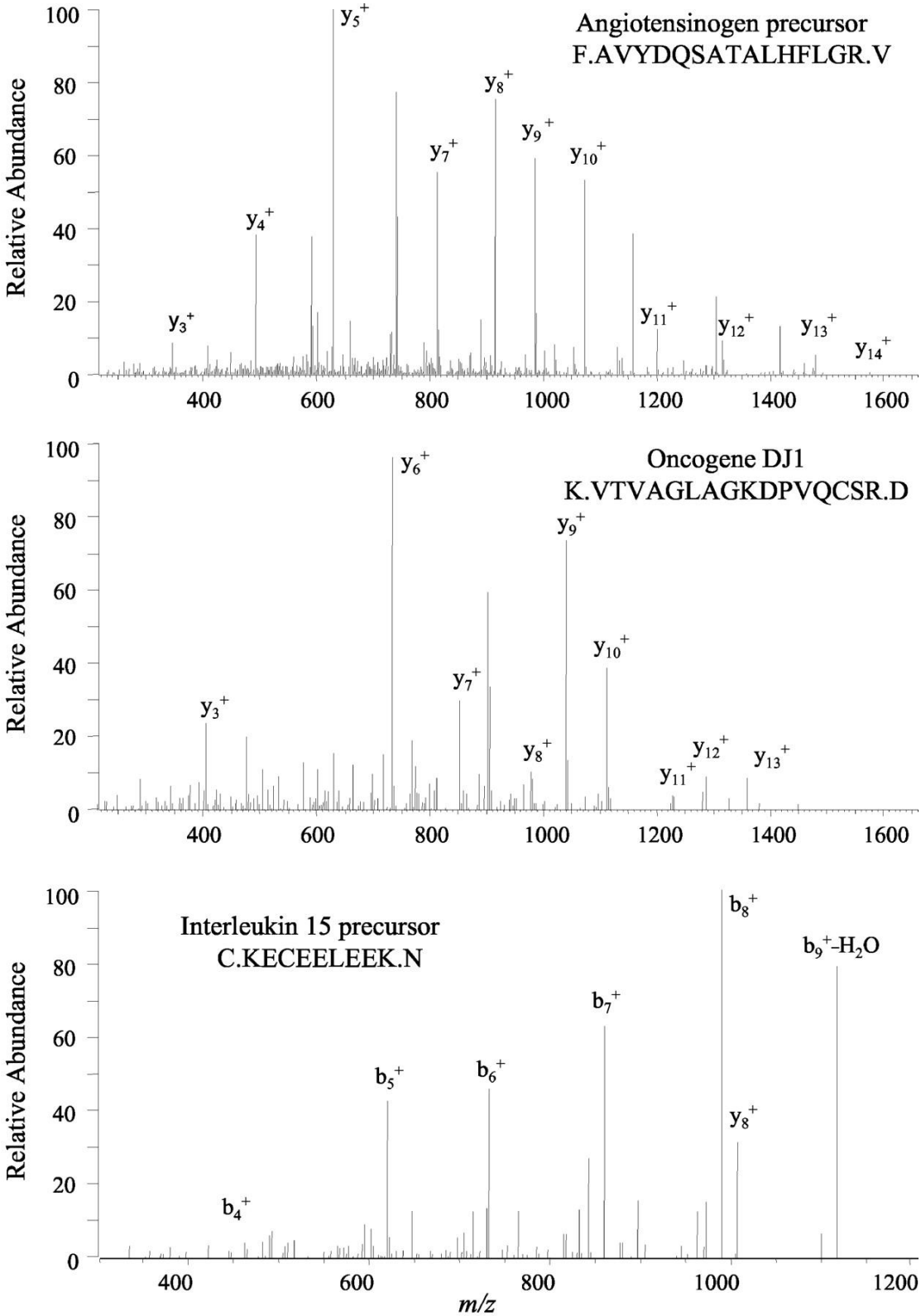

Figure 3. Tandem MS spectra of selected peptides identified in the proteome analysis of the LMW proteome. Peptide enrichment using the mesoporous silica thin film chips with pluronic surfactants (F127, P123, L121).

ISSN: 0974-5335
IJLST (2017), 10(1):1-13

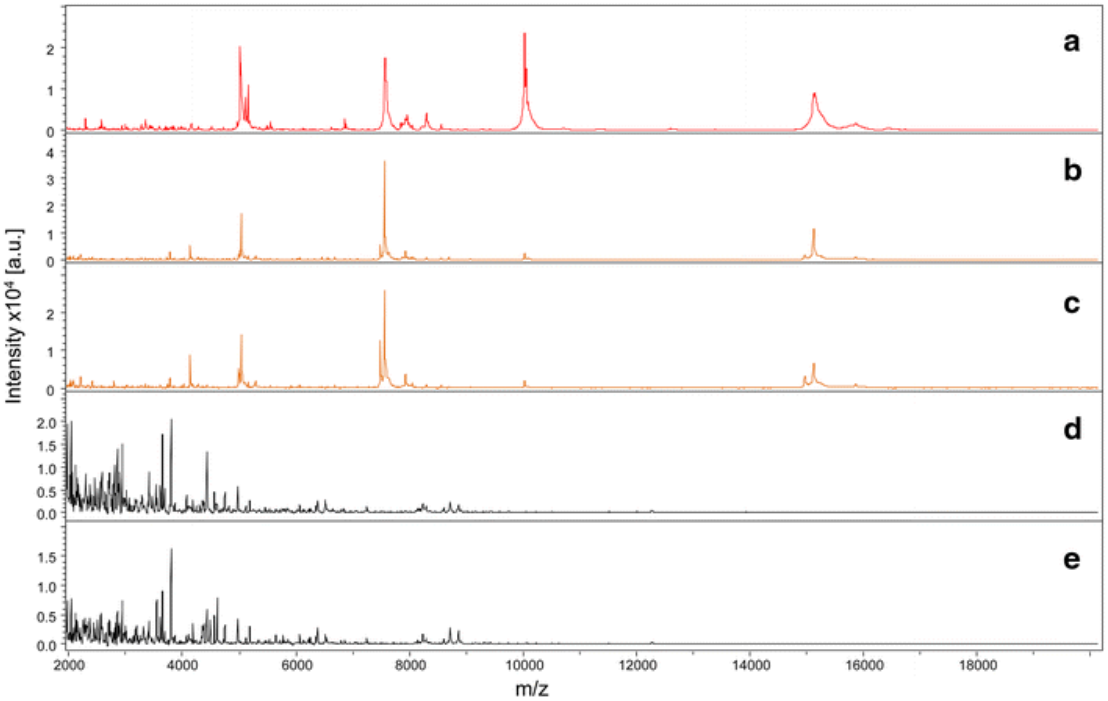

Figure 4. Peptide enrichment using the mesoporous silica thin film chips with pluronic surfactants (F127, P123, L121) with different pore sizes of (a) 6.0 nm, (b) 5.0 nm, (c) 3.0 nm, and (d) 1.0 nm, respectively. MALDI MS profiles in the mass range (2000 to 18 000 Da). (e) molecular recovery when using blank nonporous silica surfaces.

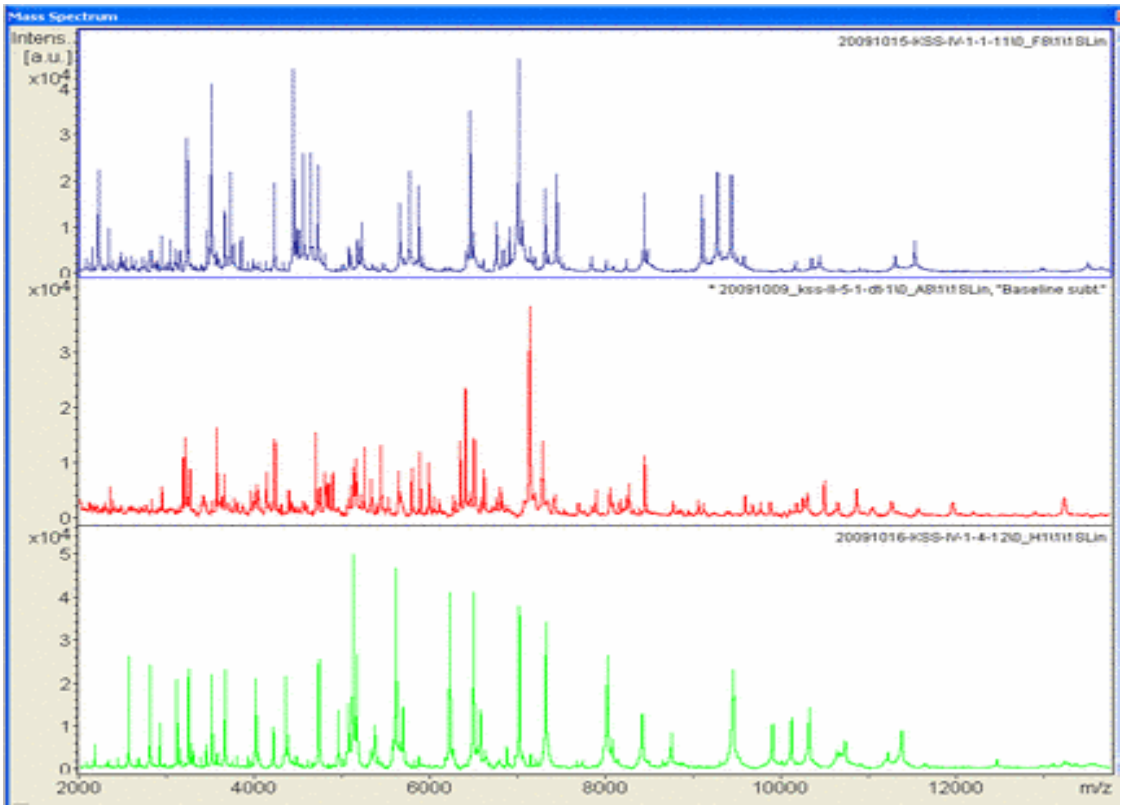

Figure 5. The recovery of LMW proteins samples from mesoporous silica thin films at different pH values, from top to bottom, pH 5.0, pH 6.0 and pH 7.0, respectively.

ISSN: 0974-5335
IJLST (2017), 10(1):1-13

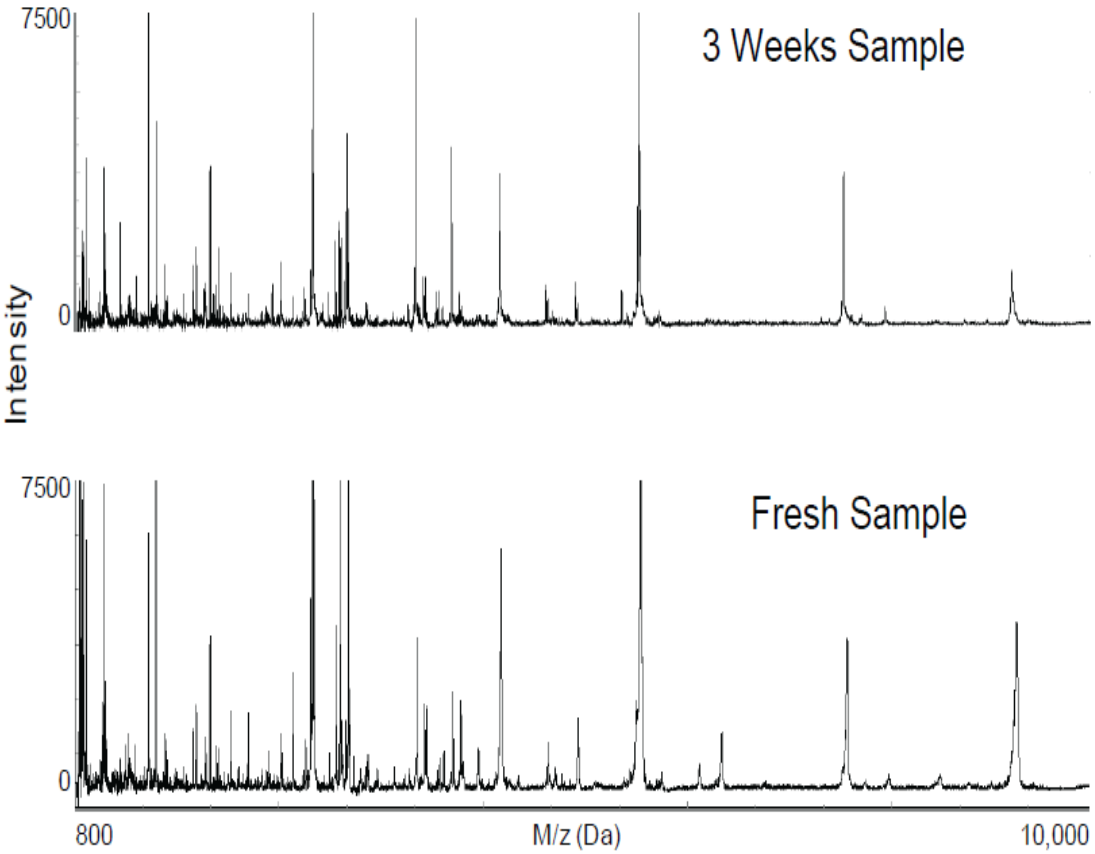

Figure 6. Stability of the LMW protein in the MPS chips with human serum, dried after washing, and stored for 3wk at room temperature.

Low abundant proteins make up about 1% of the entire human serum proteome, with the remaining 99% being comprised of only 22 proteins. It is therefore imperative to deplete the level of abundant proteins as an essential first step in the characterization of serum by MS analyses. Prefractionation approaches employing mesoporous silica thin films have been used to remove abundant proteins such as albumin, however, LMW species trapped inside the nanopores of the mesoporous silica, were preserved through the size exclusion. The method described here allows for the rapid and efficient removal of albumin and other highly abundant proteins while minimizing the concomitant loss of LMW components potentially bound to high abundant proteins. An earlier study by Georgiou et al. (26) reported that ultrafiltration failed to remove albumin and other high molecular weight proteins from human plasma. In our study the filtrate of LMW species showed a radically different profile than the serum that was applied, with no detectable albumin in the LMW species filtrate. The filtrate in our study was highly enriched for LMW proteins as shown by SDS-PAGE, SELDI-TOF MS. A detailed comparison of the conditions used in our study and that in which plasma was used shows potential reasons for this discrepancy. We diluted the serum using buffer conditions designed to disrupt protein-protein interactions, for example, thereby liberating albumin-bound species allowing them to pass through the mesoporous silica thin films. Indeed, our results illustrate the importance of using denaturing conditions, as much less enrichment for LMW proteins is observed when the ultrafiltration is conducted under nondenaturing solvent conditions. The previous study did not dilute the plasma prior to ultrafiltration. In addition, the integrity and stability of the LMW protein in the MPS chips with human serum, dried after washing, and stored for 3wk at room temperature. The patterns of results obtained were comparable with those of freshly preconcentrated LMW protein in MPS chips. As confirmed by the results of the statistical analysis showed in Figure

6b. MPS chips thereby allowing low molecular weight components to pass through the chips.

While one of the purposes of this study was to develop an efficient fractionation method to enable the identification of components of the LMW serum proteome, the list of proteins presented in the supplementary information reveals the presence of many proteins that possess molecular mass much greater than 30 kDa. For example, molecular mass of the intact version of the first protein listed in this table has a molecular mass of 309 kDa. The identification of peptides from proteins with intact masses greater than 30 kDa is primarily due to the high protease content of serum. To confirm the presence of proteins with predicted high molecular masses in the LMW serum fraction, a LMW serum filtrate was separated by SDS-PAGE and selected bands were excised and identified by MS. Indeed, peptides originating from proteins with molecular masses greater than 30 kDa were identified including kininogen (47,000 Da), apolipoprotein A-IV precursor (44,000 Da), α-2HS-glycoprotein (41,000 Da), α2 antiplasmin precursor (54,000 Da), and complement factor B precursor (84,000 Da). Therefore, it appears that the LMW proteome of serum is comprised of many proteolytic fragments from larger proteins and it cannot be assumed to be composed solely of intact proteins.

The most extensive characterization and cataloging of serum proteins to date is that 490 proteins were identified. Although nanoporous silica thin film was used to deplete immunoglobulins prior to MS analysis, six immunoglobulin proteins were identified in our study (about 2% of the total number), thus minimizing the source of repeated identification of previously well characterized proteins. Also no albumin peptides were identified, suggesting the effectiveness of ultrafiltration for nanoporous silica thin. Furthermore, only four peptides were identified as arising from haptoglobulin or transferrin, two other highly abundant serum proteins. It should to be noted that in the absence of a complete understanding of the serum proteome, much less, its LMW fraction, the presence or absence of a particular protein might be a matter of conjecture.

The overlap between the proteins identified in this study and in those conducted by Anderson et al. (27) and Adkins et al. (28) is ~11 and 16%, respectively. This low degree of overlap is not entirely surprising as there are several differences in the sample, sample preparation, and analysis in all of the compared studies. The study by Anderson et al., listed proteins from plasma that had been identified via two-dimensional-PAGE combined with MS analysis (27). The study of Adkins et al., while using a separation and MS analysis approach similar to our study, preceded with fractionation only after immunoglobulin depletion (9). The ultrafiltration-fractionation by nanoporous silica thin within our study to enrich for the LMW proteome would result in a vastly different protein content of the serum sample being analyzed.

While serum is one of the most difficult proteome samples to characterize, the ability to do so promises rich information regarding the histological state of a patient and its analysis using proteomic techniques is being counted on for the discovery of reliable disease biomarkers. Fortunately our study, as well as the one by Adkins et al., shows that the majority of proteins identified in serum are secreted or shed by cells during signaling, necrosis, apoptosis, and hemolysis. In fact a small proportion of the identified proteins are what would be thought of as classical “blood” proteins, such as cytokines, hormones, growth factors, as well as coagulation and complement factors. Some of the noteworthy proteins we have identified in serum include several oncogenes (genes that normally direct cell growth) that, if altered by heredity or environmental stress, can promote uncontrolled cell growth, as in cancer. Among the particularly interesting proteins are the 29-amino acid CRISPP peptide (cancer-associated serine protease protecting peptide), isolated earlier from plasma of cancer patients (24), a proteolytic fragment of the mut S homolog that has been associated with hereditary non-polyposis colon cancer (29), glioma pathogenesis-related protein (30), which is normally overexpressed in brain tumors, the proto-oncogene c-ets-1 (31), oncogene lbc (32), and the novel oncogene DJ1, which has been shown to interact with c-myc and also transform NIH 3T3 cells in cooperation with ras (33). In addition proteins such as the angiotensinogen precursor, the prostatic tumor suppressor Kangai-1 antigen (34), and the cytokines interleukin-15, and leukemia inhibitory factor (35), which is present in serum at a concentration below 10 pg/ml (36), were also identified.

CONCLUSION

In this work, we have demonstrated that nanoporous silica thin films (NPSTF) could be successfully employed to capture, enrich, and protect the LMWP from serum samples. The advantages in using NPSTF is obvious. The pore size

of the nanoporous silicon film could be well controlled by electrochemical etching conditions. As a result, selective sieving biomolecules with a target range of molecular size and electric charge could be readily achieved. Moreover, the LMWP captured by the NPSTF could be directly subjected to analysis by MALDI-TOF MS detection after the elution step of the LMW proteins. The nanoporous silica and technologies proposed in this work allow us conveniently fractionate LMWP from complex serum samples and acquire peptide profiles based on MS detection. Not only is reproducibility in the preconcentration and a elution step important, but reproducibility through the entire MS analysis is necessary for useful diagnostic applications of serum proteomics. Preliminary data indicates that serum from colorectal cancer patients can be nearly analysed and distinguished from those of healthy individuals based on pattern of peptides by using this type of analysis .

REFERENCES

[1] Etzioni R., Urban N., Ramsey S., McIntosh M., Schwartz S., Reid B et al. (2003) The case for early detection. Nat Rev Cancer, 3 : 243–252.

[2] Aldred S., Grant M.M., Griffiths H.R. (2004) The use of proteomics for the assessment of clinical samples in research. Clin Biochem, 37:943–952.

[3] Howard B.A., Wang M.Z., Campa M.J., Corro C., Fitzgerald M.C., Patz E.F. Jr. (2003) Identification and validation of a potential lung cancer serum biomarker detected by matrix-assisted laser desorption/ioniza-tion-time of flight spectra analysis. Proteomics , 3:1720 – 1724.

[4] Petricoin E.F., Liotta L.A. (2003) Counterpoint—The vision for a new diagnostic paradigm. Clin Chem. , 49:1276–1278.

[5] Washburn M.P., Wolters D.Yates JR . (2001) Large-scale analysis of the yeast proteome by multidimensional protein identification technology. Nat Biotechnol , 19:242–247.

[6] Pieper R, Gatlin C.L., Makusky A.J., Russo P.S., Schatz C.R., Miller S.S, et al. (2003) The human serum proteome: display of nearly 3700 chromatographically separated protein spots on two-dimensional electrophoresis gels and identification of 325 distinct proteins. Proteomics , 3:1345– 1364.

[7] Chan K.C., Lucas D.A., Hise D., Schaefer C.F., Xiao Z., Janini G.M, et al. (2004) Analysis of the human serum proteome. Clin Proteomics ,1:101–225.

[8] Peng J., Elias J.E., Thoreen C.C., Licklider L.J., Gygi S.P. (2003) Evaluation of multidimensional chromatography coupled with tandem mass spectrometry (LC/LC-MS/MS) for large-scale protein analysis: the yeast proteome. J Proteome Res , 2:43–50.

[9] Liotta L.A., Ferrari M., Petricoin E. (2003) Clinical proteomics: Written in blood. Nature , 425:905-920.

[10] Diamandis E.P. (2002) Proteomic patterns in serum and identification of ovarian cancer [Letter]. Lancet , 360:170-179.

[11] Guillaume E., Zimmermann C., Burkhard P.R., Hochstrasser D.F., Sanchez J.C. (2003) A potential cerebrospinal fluid and plasmatic marker for the diagnosis of Creutzfeldt Jakob disease. Proteomics , 3:1495–1499.

[12] Howard B.A., Wang M.Z., Campa M.J., Corro C., Fitzgerald M.C., Patz E.F. Jr. (2003) Identification and validation of a potential lung cancer serum biomarker detected by matrix-assisted laser desorption/ioniza-tion-time of flight spectra analysis. Proteomics , 3:1720 – 1724.

[13] Koopmann J., Zhang Z., White N., Rosenzweig J., Fedarko N., Jagannath S, et al. (2004) Serum diagnosis of pancreatic adenocarci-noma using surface-enhanced laser desorption and ionization mass spectrometry. Clin Cancer Res , 10:860 –868.

[14] Menon U., Jacobs I. (2002) Screening for ovarian cancer. Best Pract Res Clin Obstet Gynaecol , 16:469 – 482.

[15] Petricoin E.F., Ardekani A.M., Hitt B.A., Levine P.J., Fusaro V.A., Steinberg S.M, et al . (2002) Use of proteomic patterns in serum to identify ovarian cancer. Lancet , 359:572–577.

[16] Zheng P.P., Luider T.M., Pieters R., Avezaat C.J., van den Bent M.J., Sillevis Smitt P.A, et al . (2004) Identification of tumor-related proteins by proteomic analysis of cerebrospinal fluid from patients with primary brain tumors. J Neuropathol Exp Neurol , 62:855–862.

[17] Diamandis E.P. (2004) Mass spectrometry as a diagnostic and a cancer biomarker discovery tool: opportunities and potential limitations. Mol Cell Proteomics , 3:367–378.

[18] Omenn G.S . (2004) The Human Proteome Organization Plasma Proteome Project pilot phase: reference specimens, technology platform comparisons, and standardized data submissions and analyses. Proteomics , 4:1235– 1240.

[19] Zhang X., Leung S.M., Morris C.R., Shigenaga M.K. (2004) Evaluation of a novel, integrated approach using functionalized magnetic beads, bench-top MALDI-TOF-MS with prestructured sample supports, and pattern recognition software for profiling potential biomarkers in human plasma. J Biomol Tech , 15:167–175.

[20] Wang Y., Zhao D. (2007) On the controllable soft-templating approach to mesoporous silicates. Chem. Rev. , 107, 2821–2860.

[21] Beck J.S., Vartul J.C., Roth W.J., Leonowicz M.E., Kresge C.T., Schmitt K.D., Chu CT-W., Olsen D.H., Sheppard E.W., McCullen S.B., Higgins J.B., Schlenker J.L. (1992) A new family of mesoporous molecular sieves prepared with liquid crystal templates. J. Am. Chem. Soc. , 114, 10834–10843.

[22] Kresge C.T., Leonowicz M.E., Roth W.J., Vartuil J.C., Beck J.S. (1992) Ordered mesoporous molecular sieves synthesized by a liquid-crystal template mechanism. Nature , 359, 710–712.

[23] Zhao D., Feng J., Huo Q., Melosh N., Fredrickson G.H., Chmelka B.F., Stucky G.D. (1998) Triblock

copolymer synthesis of mesoporous silica with periodic 50 to 300 angstrom pores. Science , 279, 548–552.

[24] Sakamoto Y., Kaneda M., Terasaki O., Zhao D.Y., Kim J.M., Stucky G., Shim H.J., Ryoo R. (2000) Direct imaging of the pores and cages of three-dimensional mesoporous materials. Nature , 408, 449–453.

[25] Ravikovitch P.I., Neimark A.V. (2002) Density functional theory of adsorption in spherical cavities and pores size characterization of templated nanoporous silicas with cubic and three-dimensional hexagonal structures. Langmuir , 18; 1550–1560.

[26] Gorg A., Weiss W., Dunn M.J. (2004) Current two-dimensional electrophoresis technology for proteomics. Proteomics , 4:3665–3685.

[27] Anderson N. L., and Anderson N. G. (2002) The human plasma proteome: history, character, and diagnostic prospects. Mol. Cell. Proteomics , 1: 845– 867.

[28] Adkins J. N., Varnum S. M., Auberry K. J., Moore R. J., Angell N. H., Smith R. D., Springer D. L., and Pounds J. G. (2002) Toward a human blood serum proteome: analysis by multidimensional separation coupled with mass spectrometry. Mol. Cell. Proteomics, 1: 947– 955.

[29] Fishel R., Lescoe M. K., Rao M. R., Copeland N. G., Jenkins N. A., Garber J., Kane M., and Kolodner R. (1993) The human mutator gene homolog MSH2 and its association with hereditary nonpolyposis colon cancer. Cell , 75, 1027– 1038.

[30] Murphy E. V., Zhang Y., Zhu W., and Biggs J. (1995) The human glioma pathogenesis-related protein is structurally related to plant pathogenesis-related proteins and its gene is expressed specifically in brain tumors. Gene , 159: 131– 135.

[31] Reddy E. S., and Rao V. N. (1998) Structure, expression and alternative splicing of the human c-ets-1 proto-oncogene. Oncogene. Res. , 3: 239–246.

[32] Toksoz D., and Williams D. A. (1994) Novel human oncogene lbc detected by transfection with distinct homology regions to signal transduction products. Oncogene , 9: 621– 628.

[33] Nagakubo D., Taira T., Kitaura H., Ikeda M., Tamai K., Iguchi-Ariga S. M., and Ariga H. (1997) DJ-1 a novel oncogene which transforms mouse NIH3T3 cells in cooperation with ras. Biochem. Biophys. Res. Commun. , 231: 509– 513.

[34] Dong J. T., Lamb P. W., Rinker-Schaeffer C. W., Vukanovic J., Ichikawa T., Isaacs J.T., and Barrett J. (1995) CKAI1 a metastasis suppressor gene for prostate cancer on human chromosome 11 p11.2. Science , 268: 884– 886.

[35] Tomida M., Yoshida U., Mogi C., Maruyama M., Goda H., Hatta Y., and Inoue K. (2001) Growth hormone by rat pituitary MtT/SM cells. Cytokine , 14: 202– 207.

[36] Wegner N. T., and Mershon J. L. (2001) Evaluation of leukemia inhibitory factor as a marker of ectopic pregnancy. Am. J. Obstet. Gynecol. , 184: 1074– 1076.